

3-Hydroxy-2-methylene-3-(4-nitrophenyl)propanenitrile): A new highly active compound against epimastigote and trypomastigote form of *Trypanosoma cruzi*

Jana M. Sandes^a, Andrezza R. Borges^a, Cláudio G.L. Junior^b, Fábio P.L. Silva^b, Gabriel A.U. Carvalho^c, Gerd B. Rocha^{c,***}, Mário L.A.A. Vasconcellos^{b,**}, Regina C.B.Q. Figueiredo^{a,*}

^a Departamento de Microbiologia, Centro de Pesquisas Aggeu Magalhães, FIOCRUZ, Recife, PE, Brazil

^b LASOM-PB, Departamento de Química, Universidade Federal da Paraíba, Campus I, 58059-900 João Pessoa, PB, Brazil

^c Laboratório de Química Quântica Computacional (LQQC)-Departamento de Química, Universidade Federal da Paraíba, Campus I, João Pessoa, PB 58059-900, Brazil

ARTICLE INFO

Article history:

Received 11 February 2010

Available online 1 July 2010

Keywords:

Morita–Baylis–Hillman adducts

Anti-*Trypanosoma cruzi* activity

ABSTRACT

We have synthesized the Morita–Baylis–Hillman adduct (MBHA) 3-hydroxy-2-methylene-3-(4-nitrophenyl)-propanenitrile (**3**) in quantitative yield and evaluated on *Trypanosoma cruzi* epimastigote and bloodstream trypomastigote forms. Compound **3** strongly inhibited epimastigote growth, with IC₅₀/72 h of 28.5 μM and also caused intense trypomastigotes lysis, with an IC₅₀/24 h of 25.5 μM. Ultrastructural analysis showed significant morphological changes on both parasite forms treated with **3**, including increase of cell volume and rounding of cell body as well as intense intracellular disorganization. Morphological changes indicative of apoptosis, autophagy or necrosis were observed in most affected cells. Docking calculations of **1**, **2** and **3** pointed out the possibility of *T. cruzi* Farnesyl Pyrophosphate Synthase (TcFPPS) enzyme inhibition in **3** mechanism of action.

© 2010 Elsevier Inc. All rights reserved.

1. Introduction

Trypanosomiasis are a widespread group of parasitic diseases that affect over 100 millions of people, especially in the tropical and subtropical countries [1]. American trypanosomiasis or Chagas disease, caused by the hemoflagellate protozoan *Trypanosoma cruzi*, is a major public health concern in Latin America, with over 17 million people infected and at least 40 million individuals at risk of infection, either through contact with an insect vector or via blood transfusion [2]. Chagas disease presents an initial or acute phase with evident parasitemia seen in direct examination of the blood. In most cases there are no symptoms, but in symptomatic cases there are fever, generalized adenopathy, edema, hepatosplenomegaly, myocarditis and meningoencephalitis. This is followed by a chronic phase that in most cases presents as an indeterminate form, which may, in turn, evolve to severe cardiac or digestive disorders [3].

Introduced in the years 1960, the nitroderivative benznidazole (BZL, **1** Fig. 1) (Rochagan[®] and Rodanil[®]) and nifurtimox (Lampit[®]) are the only currently available drugs for treatment of Chagas disease in Latin America. The biochemical basis by which BZL exerts

its trypanocidal activity has not been fully elucidated, but evidence suggests that BZL could interfere with the synthesis of macromolecules via covalent binding or other types of interactions between nitroreduction intermediates and various cellular components, i.e., DNA, lipids, and proteins of *T. cruzi* [4–6]. Although being effective for acute infections, they cause severe side effects, which frequently lead to the treatment discontinuation [7]. Furthermore, the efficacy of treatment during the chronic phase is still controversial with a lack of consensus about the evaluation of parasitological cure [8,9]. Residronate (Actonel[®], **2** Fig. 1) is also an active substance against *T. cruzi* [10]. The mode of action of this bisphosphonate drug involves the inhibition of farnesyl pyrophosphate synthetase (FPPS), an enzyme from the mevalonic acid pathway [11,12].

Despite the high incidence and mortality of this illness, there has been little commercial interest in developing new trypanocidal compounds. Thus, the discovery of new trypanocidal compounds, less toxic than current drugs is still urgently needed [2].

The 3-hydroxy-2-methylene-3-(4-nitrophenyl)-propanenitrile (**3**, Fig. 1) is a very simple Morita–Baylis–Hillman adduct (MBHA) [13], which can be prepared in “one-pot” from *p*-nitrobenzaldehyde and acrylonitrile through the Morita–Baylis–Hillman reaction [14,15].

The bioactivity of **3** was first described in 1999, against *Plasmodium falciparum*, the parasite that causes malaria [16]. In 2006, the molluscicidal activities of 10 aromatic MBHA have been determined against *Biomphalaria glabrata* (Say) snails [17], the intermediate

* Corresponding author. Fax: +55 81 2101 2500.

** Corresponding author. Fax: +55 83 3216 7437.

*** Corresponding author. Fax: +55 83 3216 7437.

E-mail addresses: gbr@quimica.ufpb.br (G.B. Rocha), mllaav@quimica.ufpb.br (M.L.A.A. Vasconcellos), bressan@cpqam.fiocruz.br (R.C.B.Q. Figueiredo).

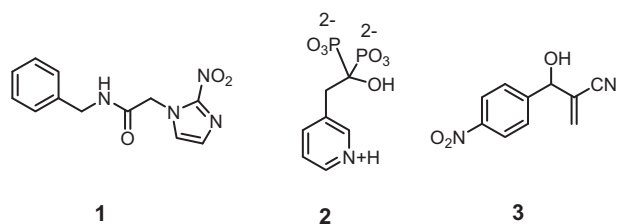


Fig. 1. Chemical structures of BZN (1), RIS (2) and (±)-3-hydroxy-2-methylene-3-(4-nitrophenyl)propanenitrile (3).

host of schistosomiasis, and in the same year, *in vitro* antiproliferative effect on human tumor cell lines were described [18]. Subsequently high *in vitro* leishmanicidal activities against *Leishmania amazonensis* [19] and *Leishmania chagasi* [20] parasites were also described for 3.

In connection with our continuum interest on organic synthesis of products with biological activity [21–25] our research group has been engaged on the development of several new conditions to produce MBHA in high yields from “one-pot reaction” [26–29], and to explore them as a new class of drugs, especially against neglected tropical diseases such as schistosomiasis [17] and leishmaniasis [19,20]. Since compound 3 has presented several important anti-parasitic activities the purpose of this article is to describe the improvement of the synthesis of 3 and to explore its biological activity against *T. cruzi* epimastigote and bloodstream trypomastigote forms, perhaps suggesting a novel drug prototype against this parasite and begin to make propositions about the compound 3 mechanism of action.

2. Materials and methods

2.1. Physical measurement

Commercially available reagents were purchased from Aldrich® and used without further purification. ¹H and ¹³C NMR spectra were obtained by using a Mercury Spectra AC 200 (200 MHz for ¹H and 50.3 MHz for ¹³C) in CDCl₃. Chromatography was made on silica gel purchased from Merck (silica gel 60, 0.063–0.200 mm). Analytical thin-layer chromatography (TLC) was carried out using 0.2 mm commercial silica gel plates (silica gel 60 with fluorescent indicator UV₂₅₄). The purity is also determined by chromatography using a RESTEK Rtx®-35MS capillary column (30 m, 0.25 mmID, 0.25 μm df) in a CG-MS/2010 (Shimadzu) equipment. Mass spectra were determined either by electronic impact (EI, 70 eV). The IR spectrum was obtained using spectrophotometer FT-IR Prestige-21 (Shimadzu). The compound 3 have been already synthesized in our previous work (75% yield, using solvent and at room temperature) [15] and characterized from NMR by comparison with the compound described in literature [20].

2.2. Improvement of the synthesis of 3

The chemical synthesis of 3 was performed through the Morita–Baylis–Hillman between the *p*-nitrobenzaldehyde (4) and acrylonitrile (5) in excess (Fig. 2), without use of solvents, at 0 °C with 100% yield. After a simple filtration the product was ready for the biological assays, which reiterates its easy handling in industrial scales.

The reaction was carried out using *p*-nitrobenzaldehyde (4) (1 mmol), 0.4 mL of acrylonitrile (5) (6 mmol) and 1 mmol of DABCO at 0 °C for 10 min. After the end of the reaction, the reaction media was directly filtered on silica gel, using AcOEt–Hexane (2:8) as solvent and the reaction product was concentrated under

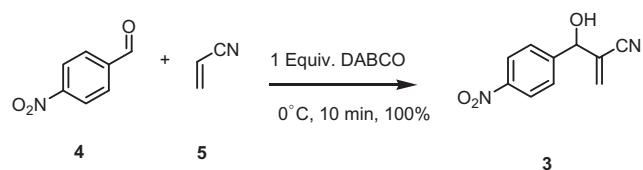


Fig. 2. Schematic representation 3 chemical synthesis (4) benzaldehyde and (5) acrylonitrile.

reduced pressure (100% yield, Fig. 2). In this new procedure, the product 3 was ready to be bioevaluated without further purification.

2.2.1. 3-hydroxy-2-methylene-3-(4-nitrophenyl)propanenitrile (3)

IR (KBr): 3447, 3115, 2228, 1599, 1520, 1348, 736 cm⁻¹; ¹H NMR (200 MHz, CDCl₃) δ 8.21 (d, *J* = 8.8 Hz, 2H); 7.58 (d, *J* = 9.0 Hz, 2H); 6.07 (d, *J* = 0.8 Hz, 1H); 6.16 (d, *J* = 0.6 Hz, 1H); 5.42 (s, 1H); 3.23 (brs, 1H, CHOH). ¹³C NMR (CDCl₃, 50 MHz): δ 73.01; 116.62; 123.92(2C); 126.13; 127.34(2C); 130.51; 146.80; 147.82. C.G.: RT = 18.410 min (100%), injection temperature = 240 °C, injection mode = split, total flow = 50 mL/min, column flow = 1.13 mL/min, O.T.P. = rate 10.00 °C/min (100–280 °C); MS: *m/e*: 152 (M⁺–CH₂=CH₂CN, 100%).

2.3. *In vitro* studies

2.3.1. Parasites

Cultures of epimastigote forms of *T. cruzi*, Dm28c clone were maintained by weekly passages at 28 °C in liver infusion tryptose (LIT) medium (Camargo, 1964), supplemented with 10% inactivated fetal bovine serum (FBS). Three-day-old culture forms were used in the experiments. Bloodstream trypomastigotes Y strain were obtained by cardiac puncture of infected Swiss albino mice, at the peak of parasitaemia (7 days post-infection). All experiments involving the use of experimental animals were performed in accordance to ethical standards of Fundação Oswaldo Cruz and were approved by ethics committee (CEUA- FIOCRUZ L-0001/08).

2.3.2. Bioactivity assay

Compound 3 (Fig. 1) was initially dissolved in dimethyl sulfoxide (DMSO) at a concentration of 50 μg/mL. This solution was then further dissolved in culture medium to obtain a stock solution at 1 mg/mL. Under these conditions, the DMSO was diluted at 2%. Both solutions were stored at –20 °C. The stock solution was then diluted in medium at 3.1–25 μg/mL so that the final concentration of DMSO never exceeded 0.05%, a nontoxic concentration to parasites. Epimastigotes (10⁶ parasites/mL) in the log phase of growth were incubated at 26 °C in LIT (liver infusion tryptose) medium supplemented with 10% FBS in the absence or presence of the different concentrations (3.1–25 μg/mL) of 3. The inhibitory effect on cell growth was then estimated by cell counting using a Neubauer chamber. Bloodstream trypomastigote were resuspended to 2 × 10⁶ in RPMI plus 10% of FBS. This suspension (100 μL) was added to the same volume of 3, previously prepared at twice the desired final concentrations. The incubation was performed in 96 well microplates at 37 °C for 24 h. The concentration that inhibited epimastigote growth by 50% (IC₅₀) and caused lysis of 50% of bloodstream trypomastigotes (IL₅₀) was determined by regression analysis using the program SPSS 8.0 for window after 72 h and 24 h of incubation respectively. All countings were performed in triplicate, in three independent experiments.

2.3.3. Ultrastructural assay

Epimastigote was incubated with corresponding IC_{50} or $2 \times IC_{50}$ and bloodstream trypomastigote forms were incubated with $2 \times IL_{50}$ and then processed for ultrastructural analysis. The parasites were fixed for 2 h at 4 °C in a solution containing 2.5% glutaraldehyde/4% paraformaldehyde in 0.1 M phosphate buffer, pH 7.2. After washing in the same buffer, the cells were post-fixed for 1 h with 1% osmium tetroxide/0.8% potassium ferricyanide/5 mM $CaCl_2$ in 0.1 M cacodylate buffer at pH 7.2. They were then dehydrated in graded acetone series and embedded for 72 h at 60 °C in PolyBed 812 resin (PolySciences, Warrington, PA, USA). Ultrathin sections were stained with 5% uranyl acetate and lead citrate and observed in a Zeiss EM109 transmission electron microscope (TEM).

2.4. Theoretical procedures

2.4.1. Molecular docking

The docking calculations were done on the Fujitsu Scigress Explorer V.7.7 platform [30], which uses the PMF force field [31] to find the best ligand pose into the binding site of TcFPDS enzyme [10]. A carbon skeleton was hand-drawn and used as a base moiety to create the structures of **3**, then we used the beautify feature of Scigress to automatically fill in the missing hydrogen atoms, determine hybridization to the atoms and standardize geometries. Even after these arrangements though, every atomic hybridization, bond and hydrogen was counted and matched against the structure at hand, in order to avoid any automatically misplaced object. Following the structure setup, single point calculations were performed

using the PM3 semiempirical method [32]. The purpose for this was to assign atomic charges for each ligand.

2.4.2. The genetic algorithm

The genetic algorithm [33] was set to a 1 kcal mol⁻¹ convergence, a 0.3 mutation rate, 5000 max generation, a seven elitism index, 0.8 crossover rate and a population size of 70 chromosomes. A number of max 300 iterations at a 0.06 rate each were set and the mean force potential of united atoms was chosen. The grid spacing was of 0.375 Å in a cubic box of 13 Å edges.

3. Results and discussion

Incubation of *T. cruzi* epimastigote forms caused a strong growth inhibition in dose and time-dependent way, with an $IC_{50}/72$ h of about 28.5 μM, reaching 100% of cell growth inhibition at 122, 4 μM. The treatment of bloodstream trypomastigote with the same compound induced intense lysis of parasites, with an $IC_{50}/24$ h value of 25.5 μM and 100% of lysis at 61 μM. The viability of treated and untreated parasites was analyzed daily by light microscopy. The treated parasites showed rounded shaped morphology with the appearance of large vacuole at nuclear region and decrease of flagellar motility (data not shown).

Epimastigote forms treated with corresponding IC_{50} or $2 \times IC_{50}$ value were also analyzed at the ultrastructural level. Control epimastigote (Fig. 3) has as main characteristics the elongated shape, a centrally located nucleus, anterior flagellum, a single large mitochondrion, which contain a large condensation of mitochondrial DNA, called kinetoplast, and reservosomes, a membrane bound

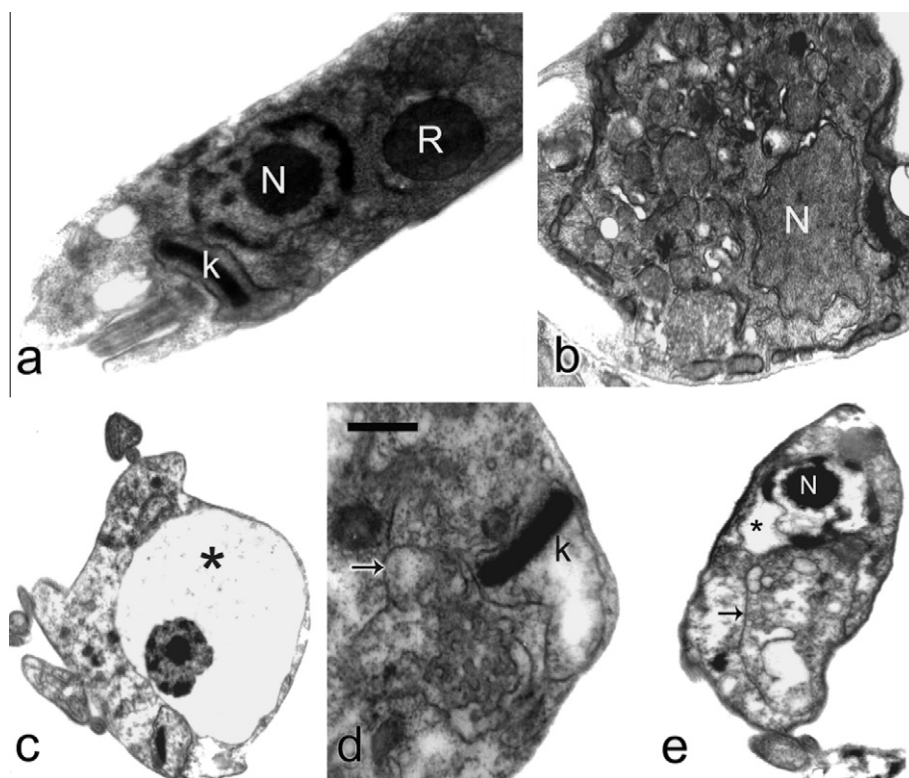


Fig. 3. Ultrastructural effects of **3** on *T. cruzi* epimastigote forms, as observed by TEM, after treatment with IC_{50} (b) or twice the corresponding IC_{50} value (c–e). (a) Untreated control epimastigote form displaying centrally located nucleus (N), the reservosomes at the posterior edge of the cell (R) and the kinetoplast (K). (b) Treated epimastigote presenting remarkable disorganization and the retraction of nuclear membrane. (c) Drastically affected cell presenting swelling of nuclear membrane with the appearance of large electron-lucent space between the nuclear monolayers, segregation of nuclear material, decrease of cytoplasm electron density and loose of cell normal morphology. (d) Detail of reticulum profiles (arrow) surrounding the partially degraded organelle. Note the reduced electron density and swelling of mitochondria close to the kinetoplast region. (e) Cell presenting condensation of chromatin, swelling of nuclear membrane and endoplasmic reticulum surrounding membranes and cytosolic structures. Bars 1 μm.

organelles which correspond to the pre-lysosomal compartments in this evolutive form. Treated epimastigotes presented several morphological changes including swelling and rounding of the parasite body and loss of internal organization, as compared with control cells (Fig. 3a–e). An interesting finding observed in most damaged cells was the swelling of nuclear envelope with appearance of a large electronlucent space between the lipidic monolayers and condensation of nuclear material, which becomes separated from nuclear membrane. (Fig. 3c). The autophagosomes which are characterized by the presence of the endoplasmic reticulum surrounding various organelles were frequently found in treated cells (Fig. 3d and e). Swelling of mitochondria with decrease of matrix electron density was eventually observed in some epimastigotes treated with twice the $IC_{50}/72$ h (Fig. 3d).

At ultrastructural level, untreated bloodstream trypomastigote forms presented elongated body, well preserved mitochondrion, homogeneous cytoplasm and a characteristic basket-shaped kinetoplast (Fig. 4a). Besides, the ultrastructural changes observed in treated-epimastigote forms, incubation of bloodstream trypomastigote with compound **3** lead to severe mitochondrial swelling with induction of intense k-DNA network disruption and eventually organelle fragmentation in the majority of cells treated with the drug (Fig. 4b). Morphological changes indicative of apoptotic process as chromatin condensation and rupture of nuclear membrane with loss of nuclear material were found in drastically damaged cell of both treated evolutive forms (Fig. 4e and c). Some cells presenting rupture of plasma membrane were also observed (Fig. 4b).

Our images obtained from the treatment of *T. cruzi* with **3** showed ultrastructural changes indicative of different cell-death pathways. Alterations such presence of endoplasmic reticulum surrounding cytoplasmic structures and autophagosome-like formations indicative of autophagy; chromatin condensation and loss of nuclear material indicative of apoptosis-like mechanisms; as well as plasma membrane rupture indicative of necrosis, were commonly observed in treated cells and have been reported in *Trypanosoma* and *Leishmania* species treated with several drugs [34,35]. In some cells, we found one or more phenotypes together, suggesting that compound **3** may be able to trigger different cell death mechanisms thought distinct signaling pathway [36].

The results obtained by electron microscopy analysis point out the nucleus as the main target of compound **3** action in both parasite forms. Again, the trypomastigote forms were more sensitive to the treatment than epimastigote forms, presenting besides the nuclear alterations, profound changes in the kinetoplast network, as well as fragmentation of mitochondria and rupture of plasma membrane. The marked swelling of mitochondria and disruption of kinetoplast network predominantly found in trypomastigote

forms, suggesting that **3** probably affect the energy metabolism in the parasite. Furthermore, the lipophilic nature of this compound may alter the mitochondrial membrane permeability leading to the organelle collapse.

The morphological changes predominantly found in trypomastigote forms, suggests that compound **3** disturbs the integrity of organelles in at least two distinct mechanisms: The first proposed mechanism is based on the studies carried out by Tonin et al. [37] who have demonstrated that the redox potential of the nitro group has influence on the trypanocidal activity. The main intermediate products responsible for the cytotoxic action of the nitrocompounds are the nitro-radical anion (NO_2^-) and hydroxylamine derivative (R-NHOH), which are produced in the reduction of the nitro group similar way to the benznidazole derivatives mechanism [37]. Therefore, the nitro group in **3** might suffer reduction and oxidize cellular constituents. Indeed, Souza et al. [19] have demonstrated that the presence of *p*-NO₂ substituent in the **3** significantly increases the toxicity against both amastigote and promastigote forms of *L. amazonensis*. The damage caused by the reaction of reduced nitro radicals with cellular constituents might lead to the activation of cell-death pathways due to damage in DNA, membranes, lipids and proteins. The second proposed mechanism suggests that the **3** may act through the inhibition of the TcFPPS enzyme, which takes part in early catalytic steps of sterols biosynthesis pathway. Specific endogenous sterols have a remarkable part in growth and development of *T. cruzi* and *Leishmania* parasites because of their participation in post-translational regulation mechanisms, especially prenylation [38] (Perez-Salas et al.), which means that sterols biosynthesis inhibitors can be very potent anti-parasitic drugs [39,40]. Such data suggests that inhibition of TcFPPS depletes the parasite stocks of these essential endogenous sterols, inducing the parasite cell death throughout apoptosis, autophagy or necrosis which ultimately leads to the morphological changes seen in Figs. 4 and 5 such as nucleus swelling, mitochondrial fragmentation with profound changes in the kinetoplast network and rupture of plasma membrane.

A complement to the experimental studies presented here, we decided to carry out a theoretical molecular docking calculation of benznidazole (Rocheagan®) (**1**), Risidronate (**2**) (Actonel®) and 3-hydroxy-2-methylene-3-(4-nitrophenyl)propanenitrile (**3**) on TcFPPS. We have chosen compounds **1** and **2** (Fig. 2) as reference chemical structures to the molecular docking calculations. First, as the molecular mechanism of benznidazole (**1**) is not the inhibition of FPPS [4–6], a non-interaction between **1** and TcFPPS is expected in docking results, which would be a form of validation of our theoretical docking methodology. Compound **2** was also selected as standard chemical structure because of its elucidated role as an inhibitor of TcFPPS and its high efficacy which ranges in nM

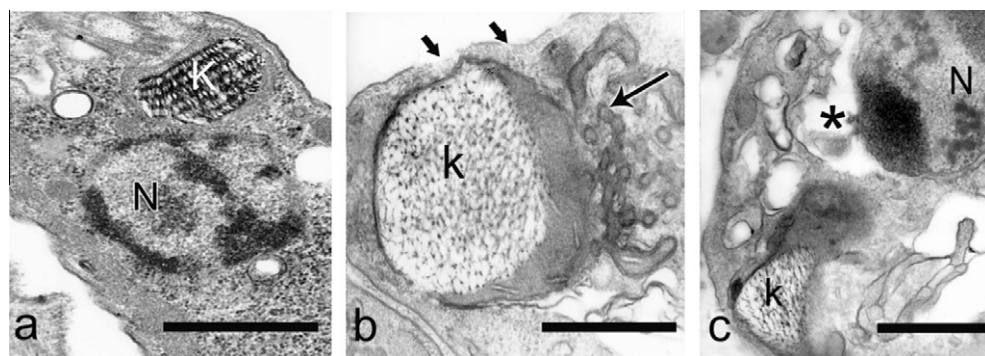


Fig. 4. Ultrastructural analysis of trypomastigote of *T. cruzi* treated with **3** (a) Untreated trypomastigote showing homogenous cytoplasm, a characteristic basket-like kinetoplast (K) and nucleus (N). (b) Compound **3** lead to swelling of mitochondria with fragmentation of organelle (long arrow), k-DNA network disruption and membrane rupture (short arrow). (c) Drastic affected cell showing swelling of nuclear membrane, disorganization of k-DNA network and cytoplasm vacuolation (V). Bars 1 μ m.

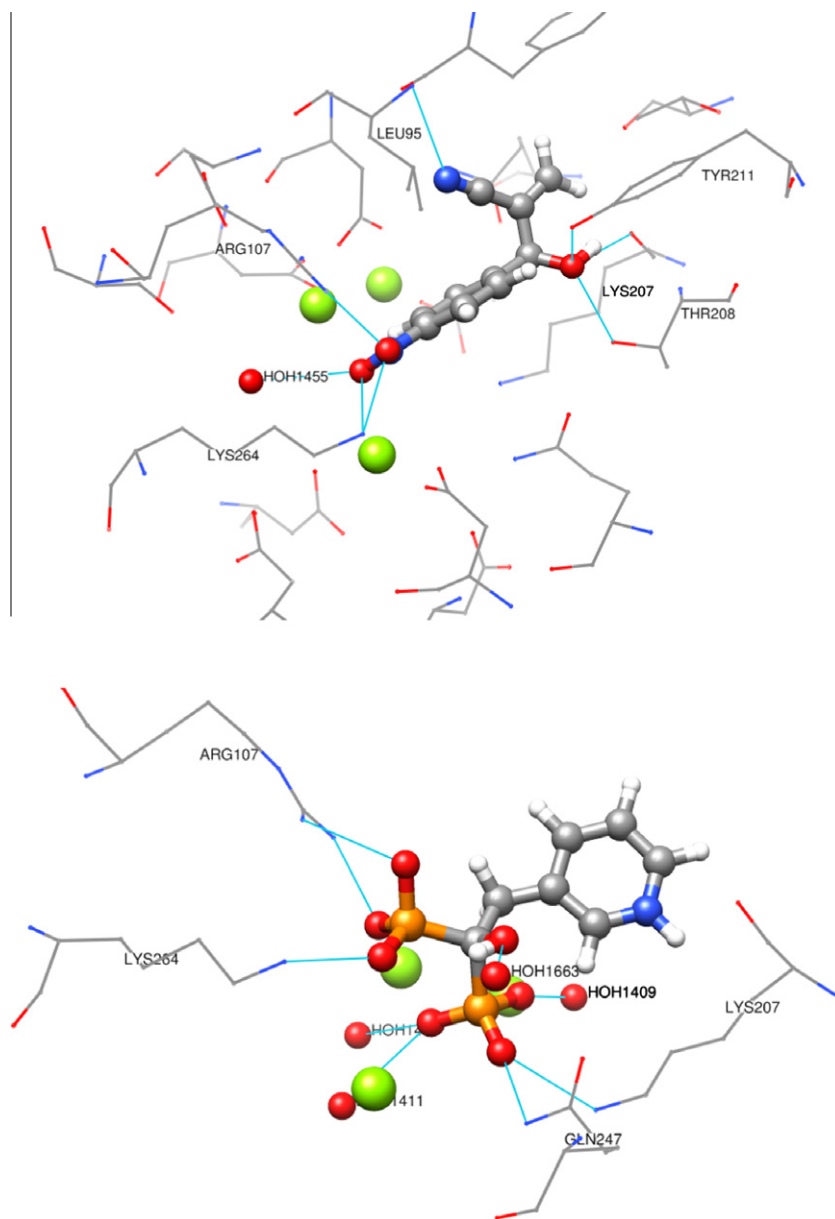


Fig. 5. (Downside) The best pose of RIS (**2**) redock in TcFPPS (in blue). The crystallographic geometry is represented in red and the active site in black. (Upside) Best pose of **3** in TcFPPS obtained by molecular docking. Hydrogen bonds are in cyan. The DMAPP residue was omitted to produce a better picture. (For interpretation of the references to colour in this figure legend, the reader is referred to the web version of this article.)

Table 1

Ligand	PMF SCORE (kcal mol ⁻¹) ^a
1	+84.297
2	-119.142
3	-77.543

^a A negative value of PMF SCORE indicate a *in silico* inhibition of TsFPPS and a positive value of PMF SCORE indicate no inhibition TsFPPS enzyme.

scales [10] and, a high affinity of **2** by the TcFPPS is also a relevant point to validate our docking calculations. Besides, since this enzyme has already been isolated, crystallized and made available in PDB database (1YHL, <http://www.rcsb.org/pdb/home/home.do>), it seemed a good starting point to perform molecular docking [41,42] in order to propose a molecular target for **3**. The docking

score of each one of the ligands **1**, **2** and **3** was then compared to one another. These results are shown in Table 1.

From the docking calculations results (Table 1) we notice that, in fact, Risidronate (**2**) is the most active molecule as a TcFPPS inhibitor, which is in agreement with its experimental nM efficacy scale [41,42]. Also as expected, the benzimidazole (**1**) score was very positive, which also agrees with experimental data pointing it does not work as a TcFPPS inhibitor [4–6]. These results validate our docking methodology. By this approach, the 3-hydroxy-2-methylene-3-(4-nitrophenyl)propanenitrile (**3**) showed a negative PMF score, suggesting that they may play, at least in part, a role as TcFPPS inhibitors, however in a lesser extend when compared with RIS (**2**) as expected (Table 1). The best poses of **2** and **3** in TcFPPS obtained by molecular docking are presented in Fig. 5.

We can see compound **3** has formed eight H-bonds. Four hydrogen bonds were identified at the nitro group: two with the side chain of ARG107, one with LYS264 and one with the crystal water

molecule HOH1455; three in the hydroxyl group: one with TYR211, one with ASP170 and one with the hydroxyl at THR208 and the last between the nitrile group and ASP98.

As for RIS (**2**), it was revealed that it forms nine hydrogen bonds with residues of the active site of TcFPPS. One at the hydroxyl group and the other eight at the phosphate groups (Fig. 5). Furthermore, distances comparable to coordination bonds were detected between **2** phosphate groups and the magnesium ions coordinated with TcFPPS active site aminoacids.

In conclusion, we envisioned that the molecule **3**, might have an enormous potential as drug candidate in the Chagas disease treatment. This statement is supported primarily by the expected simplicity and efficiency associated with its synthesis (having functional groups as diverse as a double bond, a nitro group, a hydroxyl group, and an aryl group). It is also important to emphasize that compound **3** was easily prepared at one-pot reaction, in 10 min and obtained in 100% yield. After a simple filtration the product was ready for the biological assays, which reiterates its easy handling in industrial scale. On the other hand, our data has shown that **3** was active against *T. cruzi* epimastigotes and trypomastigote forms, exhibiting a remarkable *in vitro* trypanocidal activity at a μM scale.

Acknowledgments

This work has been supported by CNPq, CAPES, FAPESQ-PB, FIOCRUZ, The authors thanks Mr. Raimundo Nazareno C. Pimentel for technical assistance. Molecular graphics images were produced using the UCSF Chimera package from the Resource for Biocomputing, Visualization, and Informatics at the University of California, San Francisco (supported by NIH P41 RR-01081).

Appendix A. Supplementary material

Supplementary data associated with this article can be found, in the online version, at doi:10.1016/j.bioorg.2010.06.003.

References

- [1] <<http://www.who.int/tdr/diseases/chagas/>> (accessed 10.01.10).
- [2] J.R. Coura, S.L. de Castro, Mem. Inst. Oswaldo Cruz 97 (2002) 3–24.
- [3] A. Prata, Lancet Infect. Dis. 1 (2001) 92–100.
- [4] E. G.D. de Toranzo, J.A. Castro, B.M. Franke de Cazzullo, J.J. Cazzullo, Experientia 44 (1998) 880.
- [5] R. Do Campo, Chem. Biol. Interact. 73 (1990) 1.
- [6] E. Piaggio, J. Sancéau, S. Revelli, O. Bottasso, J. Wietzerbin, E. Serra, J. Immunol. 167 (2001) 3422–3426.
- [7] R. Viotti, C. Vigliano, B. Lecoco, M.G. Alvarez, M. Petti, G. Bertocchi, A. Armenti, Expert Rev. Anti Infect. Ther. 7 (2009) 157–163.
- [8] S.L. Croft, Parasite 15 (2008) 522–527.
- [9] J.A. Urbina, R. do Campo, Trends Parasitol. 9 (2003) 495–501.
- [10] S.B. Gabelli, J.S. McLellan, A. Montalvetti, E. Oldefield, R. Docampo, L.M. Amzel, Proteins: Struct. Funct. Bioinf. (2006) 62 80–88.
- [11] J.M.J. Rogers, S. Gordon, H.L. Belford, F.P. Coxon, S.P. Luckman, J. Monkkonen, J.C. Frith, Cancer 88 (2000) 2961–2978.
- [12] E. Dunfort, K. Thomsson, F.P. Coxon, F.P. Lucman, F.M. Hahn, C.D. Poulter, F.H. Ebetino, M.J. Roger, J. Pharmacol. Exp. Ther. 296 (2001) 235–242.
- [13] D. Basavaiah, J. Rao, T. Satyanarayana, Chem. Rev. 103 (2003) 811–891.
- [14] A.B. Baylis, M.E.D. Hillman, German Patent 2155113, Chemical Abstracts, vol. 77, 1972, p. 34174q.
- [15] R.O.M.A. de Souza, M.L.A.A. Vasconcellos, Syn. Commun. 33 (2003) 1383–1399.
- [16] M.K. Kundu, N. Sundar, S.K. Kumar, S.V. Bhat, S.V.N. Biswas, Bioorg. Med. Chem. Lett. 9 (1999) 731–736.
- [17] M.L.A.A. Vasconcellos, T.M.S. Silva, C.A. Camara, R.M. Martins, K.M. Lacerda, H.M. Lopes, V.L.P. Pereira, R.O.M.A. de Souza, L.T.C. Crespo, Pest Manage. Sci. 62 (2006) 288–296.
- [18] L.K. Kohn, C.H. Pavam, D. Veronense, F. Coelho, J.E. De Carvalho, W.P. Almeida, Eur. J. Med. Chem. 41 (2006) 738–744.
- [19] M.L.A.A. Vasconcellos, R.O.M.A. de Souza, V.L.P. Pereira, B. Rossi-Bergmann, M.F. Muzitano, Eur. J. Med. Chem. 42 (2007) 99–102.
- [20] T.C. Barbosa, C.G. Lima Junior, F.P.L. Silva, H.M. Lopes, L.R.F. Figueiredo, S.C.O. Souza, G.N. Batista, T.G. Silva, T.M. Silva, M.R. Oliveira, M.L.A.A. Vasconcellos, Eur. J. Med. Chem. 44 (2009) 1726–1730.
- [21] L.S. Miranda, M.L.A.A. Vasconcellos, Synthesis (2004) 1767–1770.
- [22] L.S.M. Miranda, B.G. Marinho, S.G. Leitão, E.M. Matheus, P.D. Fernandes, M.L.A.A. Vasconcellos, Bioorg. Med. Chem. Lett. 14 (2004) 1573–1575.
- [23] L.S.M. Miranda, B.A. Meireles, J.S. Costa, V.L.P. Pereira, M.L.A.A. Vasconcellos, Synlett (2005) 869–871.
- [24] R.O.M.A. de Souza, B.A. Meireles, L.S. Sequeira, M.L.A.A. Vasconcellos, Synthesis (2004) 1595–1600.
- [25] U.F.L. Filho, S. Pinheiro, M.L.A.A. Vasconcellos, P.R.R. Costa, Tetrahedron Asymmetry 5 (1994) 1219–1220.
- [26] R.O.M.A. de Souza, A.L.F. Souza, T.L. Fernandez, A.C. Silva, V.L.P. Pereira, P.M. Esteves, M.L.A.A. Vasconcellos, O.A.C. Antunes, Lett. Org. Chem. 5 (2008) 379–382.
- [27] R.O.M.A. de Souza, V.L.P. Pereira, P.M. Esteves, M.L.A.A. Vasconcellos, Tetrahedron Lett. 49 (2008) 5902–5905.
- [28] R.O.M.A. de Souza, M.L.A.A. Vasconcellos, Catal. Commun. 5 (2004) 21–24.
- [29] E.B.A. Filho, E. Ventura, S.A. do Monte, B.G. Oliveira, C.G.L. Junior, G.B. Rocha, M.L.A.A. Vasconcellos, Chem. Phys. Lett. 449 (2007) 336–340.
- [30] Scigress Explorer v.7.7, Fujitsu, Tokyo, Japan, 2008.
- [31] I. Muegge, Y. Martin, J. Med. Chem. 42 (1999) 791–804.
- [32] J.J.P. Stewart, J. Comput. Chem. 10 (1989) 209.
- [33] G.M. Morris, D.S. Goodsell, R.S. Halliday, R. Huey, W.E. Hart, R.K. Belew, A.J. Olson, J. Comput. Chem. 19 (1998) 1639–1662.
- [34] R.F. Menna-Barreto, G.A. Laranja, M.C. Silva, M.G. Coelho, M.C. Paes, M.M. Oliveira, S.L. de Castro, Parasitol. Res. 103 (2008) 111–117.
- [35] N.K. Verma, G. Singh, C.S. Dey, Exp. Parasitol. 116 (2007) 1–13.
- [36] R.F. Menna-Barreto, K. Salomão, A.P. Dantas, R.M. Santa-Rita, M.J. Soares, H.S. Barbosa, S.L. de Castro, Micron 40 (2009) 157–168.
- [37] L.T.D. Tonin, V.A. Barbosa, C.C. Bocca, E.R.F. Ramos, C.V. Nakamura, W.F. da Costa, E.A. Basso, T.U. Nakamura, N.H. Sarragiotto, Eur. J. Med. Chem. 44 (2009) 1745–1750.
- [38] D. Perez-Sala, Front. Biosci. 12 (2007) 4456–4472.
- [39] J.A. Urbina, J.L. Concepcion, S. Rangel, G. Visbal, R. Lira, Mol. Biochem. Parasitol. 125 (2002) 35–45.
- [40] J.A. Urbina, Parasitology 114 (1997) S91–S99.
- [41] M. Prasenjit, V. D Prashant, S. Anuradha, B.L. Tekwani, M.A. Avery, J. Chem. Inf. Model. 48 (2008) 1026–1040.
- [42] J. Mao, S. Mukherjee, Y. Zhang, R. Cao, J.M. Sanders, Y. Song, Y. Zhang, G.A. Meints, Yi G. Gao, D. Mukkamala, M.P. Hudock, E. Oldfield, J. Am. Chem. Soc. 128 (2006) 14485–14497.